

Búzios oil field PSDM seismic spectrum analysis applied to frequency attenuation study: preliminary results

David Fraga Freitas¹, Marco Cetale¹, Luiz Alberto Santos^{1,2}, Alberto G. de Figueiredo Jr. ¹, ¹UFF/DOT/GISIS (RJ – Brazil), ²Petrobras.

Copyright 2021, SBGf - Sociedade Brasileira de Geofísica

This paper was prepared for presentation during the 17th International Congress of the Brazilian Geophysical Society held in Rio de Janeiro, Brazil, 16-19 August 2021.

Contents of this paper were reviewed by the Technical Committee of the 17th International Congress of the Brazilian Geophysical Society and do not necessarily represent any position of the SBGf, its officers or members. Electronic reproduction or storage of any part of this paper for commercial purposes without the written consent of the Brazilian Geophysical Society is prohibited.

Abstract

Pre-salt reservoirs of Búzios oil field are overlaid by a thick and complex sedimentary package (3500-4000m) which causes important scattering and severe attenuation of seismic signal. The present work performs a spectral analysis of a 3D Kirchhoff Pre-Stack Depth Migration (PSDM) seismic data from Búzios field, investigating the frequency content variation vertically and horizontally, to better understand the frequency attenuation process as the seismic wave travels through the sediments from the sea bottom down to the reservoir base in this area. To perform the spectral analysis in frequency domain, the PSDM volume was converted to time domain using the same interval velocity volume used to depth-migrate the data. The variation of frequency band as the signal propagates through the sediment package was analyzed dividing a crossline section in 12 layers of 200 ms each, from sea bottom down to the base of pre-salt reservoir formations (2700 to 5000 ms). Preliminary results suggest that most part of higher frequency loss has been occurred in post-salt package, specifically from 3600 to 3800 ms. This fact may be an indication of strong viscoelastic behavior of this interval. After that, higher frequency content is lost slowly from 3800ms down to the last layer located inside pre-salt formation. Very slight frequency spectrum variation between 4200 ms to 5000 ms indicates elastic behavior of the salt formation and underlying pre-salt formation in this interval.

Introduction

Today, the Pre-salt oil fields from SE of Brazilian continental margin are one of the most important exploration frontiers in the World. Since 2006, when the first occurrence of oil was proved in Tupi oil field, a number of giant Pre-Salt fields were discovered in Santos Basin. In this sense, Búzios field deserves highlight as it is the largest deep water oil field in the world and very productive, responding alone for 17% of the Brazilian oil production in the pre-salt.

Búzios oil field is located at central portion of Santos Basin, the largest Brazilian offshore basin. Santos Basin is a classical passive margin basin. It was developed on the geological context of the breakup of Gondwana and subsequent opening of the South Atlantic Ocean (White

and McKenzie, 1989). Its lithostratigraphy is composed by three megasequences: 1) rift; 2) post-rift and 3) drift or sag (Moreira et al. 2007).

The large crustal thinning which occurred during the rift process and subsequent important thermal subsidence of the crust in the area of Santos Basin have formed enormous space for sediments deposition. Then, associated with a huge sediment supply, a large sedimentary package has been formed. In the area of Búzios field, the economic basement depth can reach approximately 7500m. The Pre-salt reservoirs are found 5500-6000m deep, below a thick salt layer, deformed as domes of complex geometries that can reach more than 2000m of thickness (Figure 1). The Pre-salt reservoirs are characterized by rift and post-rift carbonate deposits of two main types: microbial limestones from Barra Velha Fm. (post-rift) and Coquinas from Itapema Fm (rift) (Moreira et al. 2007).

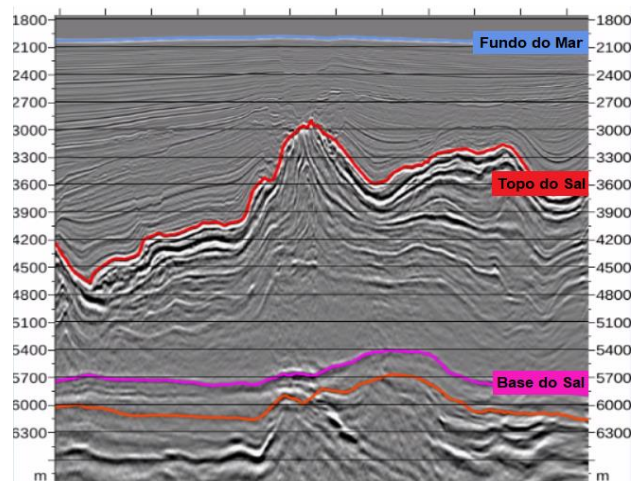


Figure 1: Interpreted seismic section from a crossline of Búzios field. Note the large sedimentary package and the huge salt wall more than 2000 m thick.

The pre-salt reservoirs of Buzios oil field lay at very deep depths, overlaid by a thick and complex sedimentary package (3500-4000m) with highly reflexive layers (e.g. clastic-salt and salt-carbonate interfaces). Thus, when the waves travel through this package most part of the seismic signal is scattered and attenuated, suffering severe amplitude reduction and losses of higher frequencies content (Figure 1). As a consequence, the seismic images at reservoir depths present reflectors with poor coherency and low resolution, what lead to uncertainties in depth and layer thickness estimation, as

well as in extension estimation, continuity and volume of reservoirs. The significant loss of higher frequencies as the wave propagates through the sediments shows that the medium is not perfectly elastic. If the medium is not perfectly elastic, the seismic signal undergoes some dissipation, as part of the energy is irreversibly converted into heat (Levergne, 1986). This process is called absorption and it is related to the frequency of the waves and, as a rule in the sediments, the higher the frequency, the greater the absorption (Levergne, 1986).

The presence of fluids in the pore space of rocks causes attenuation and dispersion mainly by the mechanism known as wave-induced fluid flow (WIFF) (Müller et al. 2010). Consequently, if attenuation depends on the fluids filling the pores and pore space, thus it depends on lithology and depth of burial. This statement have been confirmed by a number of studies based on laboratory experiments and theoretical models. They have shown that inelastic attenuation in sedimentary rocks is strongly dependent on grain size, porosity, permeability, fluid content and confining pressure at sonic-to-ultrasonic frequency (Toksöz et al. 1979; Klimentos, T. and McCann, C., 1990; Prasad and Meissner, 1992; Best and McCann, 1995) and seismic frequency bands (Pride et al. 2004; Batzle et al. 2005; Madonna et al., 2010; Tisato et al. 2011; Kuteynikova et al., 2012; Piane et al., 2014). In the case of shales, the amount of intrinsic attenuation also depends on bedding direction (Piane et al., 2014).

In this sense, the present work performs a spectral analysis of a Pre-stack Depth Migration (PSDM) seismic data from Buzios field. We investigate the frequency content variation vertically and horizontally, to understand the attenuation process as the seismic wave travels through the sediments from the sea bottom down to the reservoir base in this area. With this analysis we may have a better understanding of the signal frequency loss and mainly where and how fast this process occurs.

Method

The PSDM (Pre-Stack Depth Migrated) seismic data from Buzios field used in this study was acquired from National Petroleum Agency Database (BDEP – ANP). The processing report shows no mention to inverse Q filter to recover high frequency losses. As this data is in depth domain, to perform the spectral analysis in frequency domain, the PSDM volume was converted to time domain using the same interval velocity volume used to depth-migrate the data (Figure 2).

The spectral analysis has been conducted in the time-domain seismic obtained, using the Spectrum Analysis tool from Section application of Epos software (Emerson-Paradigm). The variation of frequency band as the signal propagates through the sediment package was analyzed dividing a crossline section in 12 layers from sea bottom down to the base of the pre-salt reservoir formation (2700 to 5000 ms) (Figure 3). The first layer, which contains the first reflections – including the sea bottom reflection – is 100 ms high. The following layers are 200 ms high (Figure 3). The first layer is intentionally thinner with the objective of capturing a frequency band as close as possible to the frequency band of the seismic signal when it reaches the sea floor. In each layer, three windows with

the same height, but different width (10, 30 and 85 traces), were used to extract the frequency band from different horizontal ranges to verify variations in frequency content in horizontal direction (Figure 3).

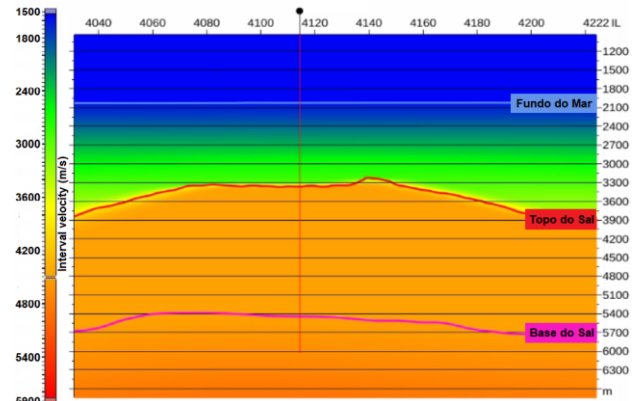


Figure 2: Interval velocity model (in depth) used to convert PSDM seismic to time domain (same model used to depth-migrate PSDM seismic).

To do that, the frequency band of the three windows with different length from the same layer are compared to each other.

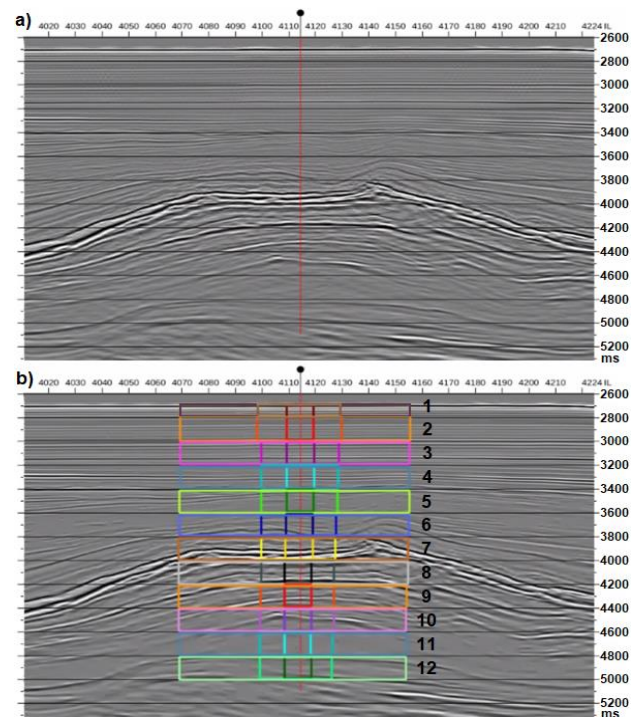


Figure 3: Seismic crossline in time domain used to perform the spectral analysis. a) crossline without analysis windows; b) same crossline with the 12 layers and respective windows of analysis. Each layer presents 3 windows of different width (10, 30 and 85 traces).

To verify the frequency content variation in vertical direction (as the seismic wave propagates from the sea floor down to the reservoir formation), the frequency band from an upper window is compared to the frequency band of the window below.

Results

The first layer (close to the sea bottom) shows a frequency band with significant signal between 4 and 75 Hz, with frequency peak at 45Hz (Figure 4). No significant frequency content variation has been observed at higher frequency range (> 25Hz) comparing frequency spectrum of different window widths, but moderate frequency variation has been shown among the different windows at lower frequency range (between 0 – 20Hz), showing some variation in horizontal direction (Figure 4). In this study we have assumed it is the seismic signal frequency band when the wave reaches the sea floor.

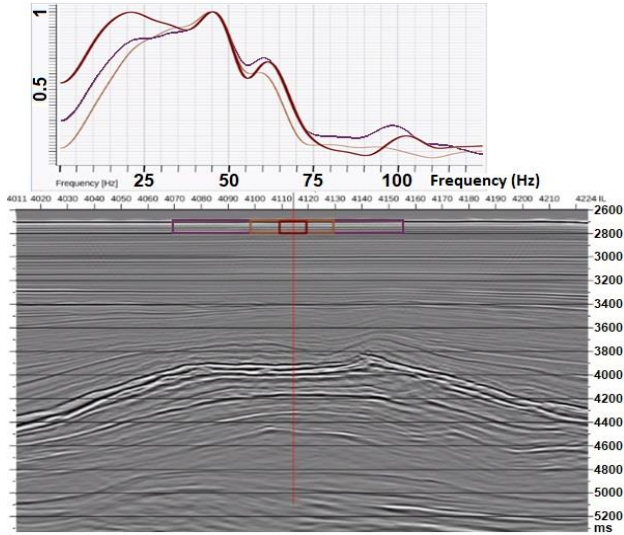


Figure 4: Normalized frequency spectrum of the 3 analysis windows of different widths (10, 30 and 85 traces) for the first layer and the analyzed seismic section in time domain. The colors spectrum curves correspond to the colors of respective analysis window. Note the location of the 1st layer analysis windows over the seismic close to the sea bottom.

Comparing the frequency bands of the first layer and the second layer one can observe significant loss of lower frequencies (4 – 30Hz) as the signal passes from the upper layer to layer 2 (Figure 5a). Few higher frequency loss is observed from 1st to 2nd layer (vertical direction). No significant frequency variation is verified through horizontal direction (among windows of different widths) in layer 2.

Passing from layer 2 to layer 3 (3000 to 3200 ms), the frequency peak is slightly dislocated to lower frequency direction in 3rd layer spectrum, but little broadening of the frequency band is observed in this layer (Figure 5b). Again, no frequency variation is observed among windows of different widths in the 3rd layer (Figure 5b).

From layer 3 to layer 4 (3200 to 3400 ms), no significant frequency loss has occurred in the main part of the signal, but a secondary low frequency peak observed in both 2nd and 3rd layers has been disappeared in the 4th layer (light blue curves, Figure 5c). Despite that, frequency spectrum from 2nd, 3rd and 4th layer are similar.

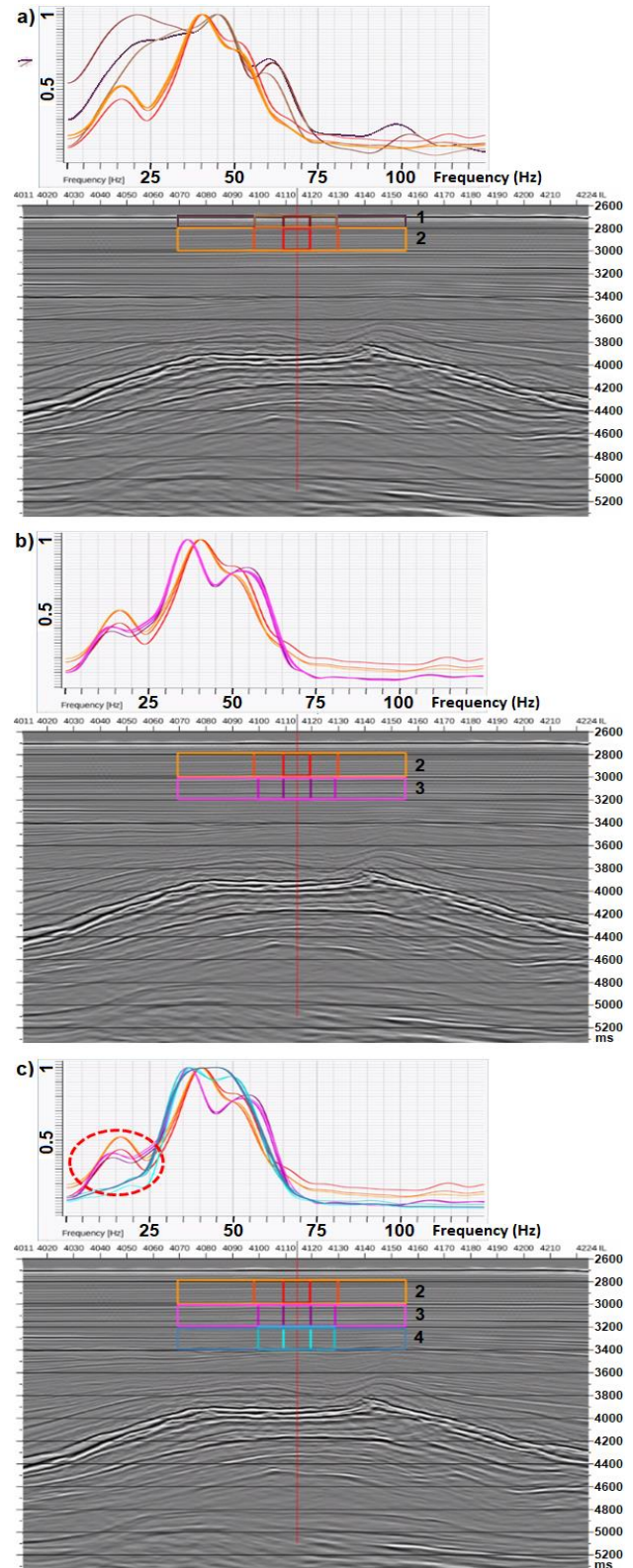


Figure 5: Normalized frequency spectrum comparing the frequency bands from: a) layer 2, b) layer 3 and c) layer 4. For each layer, frequency bands of 3 analysis windows of different widths (10, 30 and 85 traces) are calculated. The positions of the windows are marked over the analyzed seismic section in time domain.

No frequency variation was observed in horizontal direction in the layer 4 (Figure 5c).

From 4th to 5th layer, no significant frequency loss has occurred in the main part of the signal. Part of the secondary low frequency peak that has been disappeared in the layer 4 (light blue curves, Figure 6a) seems to be recovered in the layer 5 (green curves, Figure 6a). In general, frequency spectrum of 5th layer keeps similar to 2nd, 3rd, 4th layer spectrum. No frequency variation was observed in horizontal direction at layer 5 (3400 to 3600 ms).

Passing from layer 5 to layer 6 (darker blue curves, Figure 6b), a great loss of higher frequency content is observed, where the maximum frequency peak is shifted from 50Hz to 30Hz (black arrow, Figure 6b). No significant frequency variation is seen in horizontal direction in the 6th layer (3600 to 3800 ms).

The layer 7 comprehends the transition between the post-salt sediments and the salt top (3800 to 4000ms, Figure 6c). Moderate higher frequency loss is observed in vertical direction from the 6th (darker blue curves) to the 7th layer (yellow to light brown curves). The layer 8 (4000 to 4200ms) is completely inside the salt dome. A small higher frequency loss is observed from the 7th to the 8th layer (vertical direction). No significant frequency band variation is observed in horizontal direction in both 7th and 8th layers (Figure 6c).

From the layer 8 to the layer 9 (4200 to 4400ms, Figure 7a), we verify a significant recovery of higher frequencies (orange to red curves into blue dashed circle) in the deeper layer. At layer 9, the windows with different widths (horizontal direction) shows a moderate variation in low frequency band, but no significant higher frequency band variation has been observed (Figure 7a).

Still into the salt dome, a small displacement of the frequency peak followed by a broadening of frequency band in direction to lower frequencies has been verified passing from the 9th to the 10th layer (4400 to 4600ms, Figure 7b). No significant frequency band variation is observed in horizontal direction in layer 10 (purple to pink curves, Figure 7b).

Layer 11 is the last layer inside the salt dome. Its base is close to the salt base. Layer 12 is the first layer inside pre-salt formation. From the 10th to the 12th layer (4600 to 5000 ms), slight high frequency loss has been observed from layer 10 (pink to purple curves, Figure 7c) to the layer 11 (light blue curves, Figure 7c) and no significant frequency loss has been verified between the 11th and 12th layers spectra (green curves, Figure 7c). No significant frequency variation in horizontal direction has been observed in both layers 11 and 12.

As expected, all layers frequency bands are observed in the first layer frequency band. It is important to validate the assumption that first layer signal is the same of that one which reaches the sea floor.

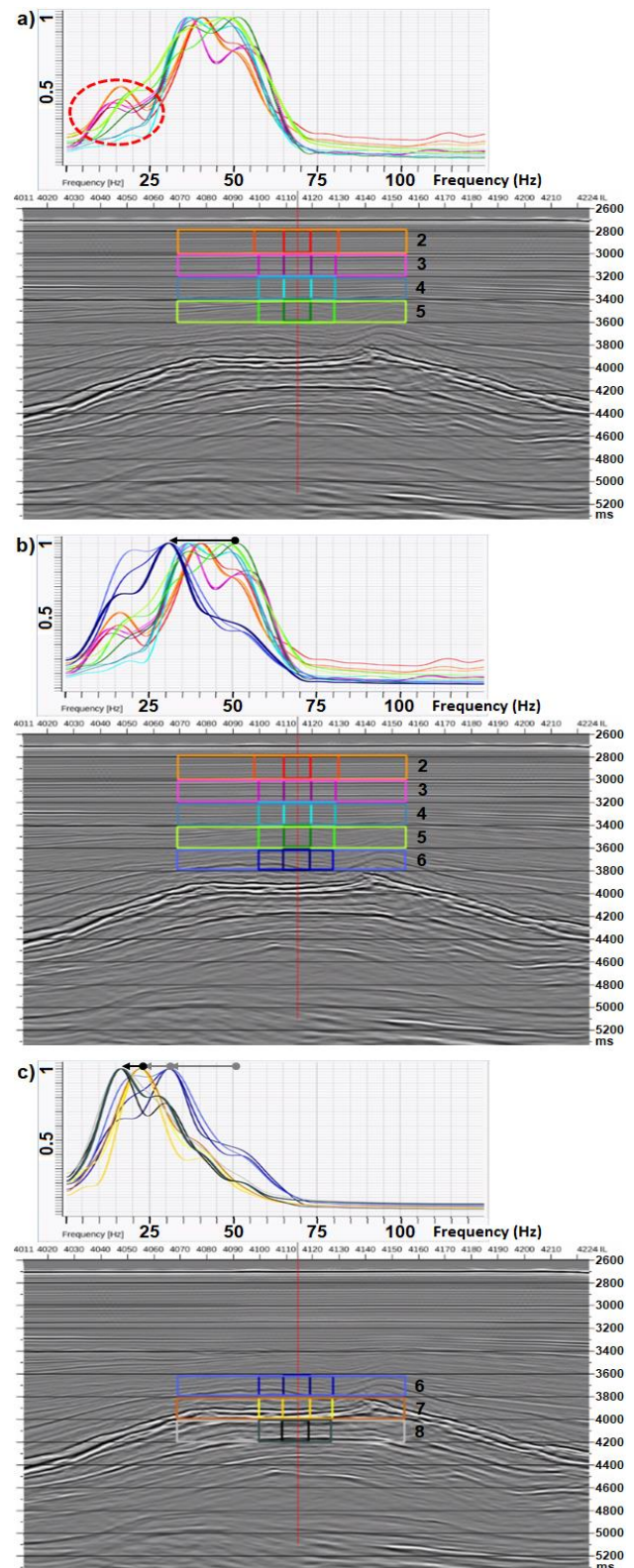


Figure 6: Normalized frequency spectrum comparing the frequency bands from: a) layer 2, 3, 4 and 5; b) layer 2, 3, 4, 5 and 6; and c) layer 6, 7 and 8. For each layer, frequency bands of 3 analysis windows of different widths (10, 30 and 85 traces) are calculated. The windows position are marked over the TWT seismic section.

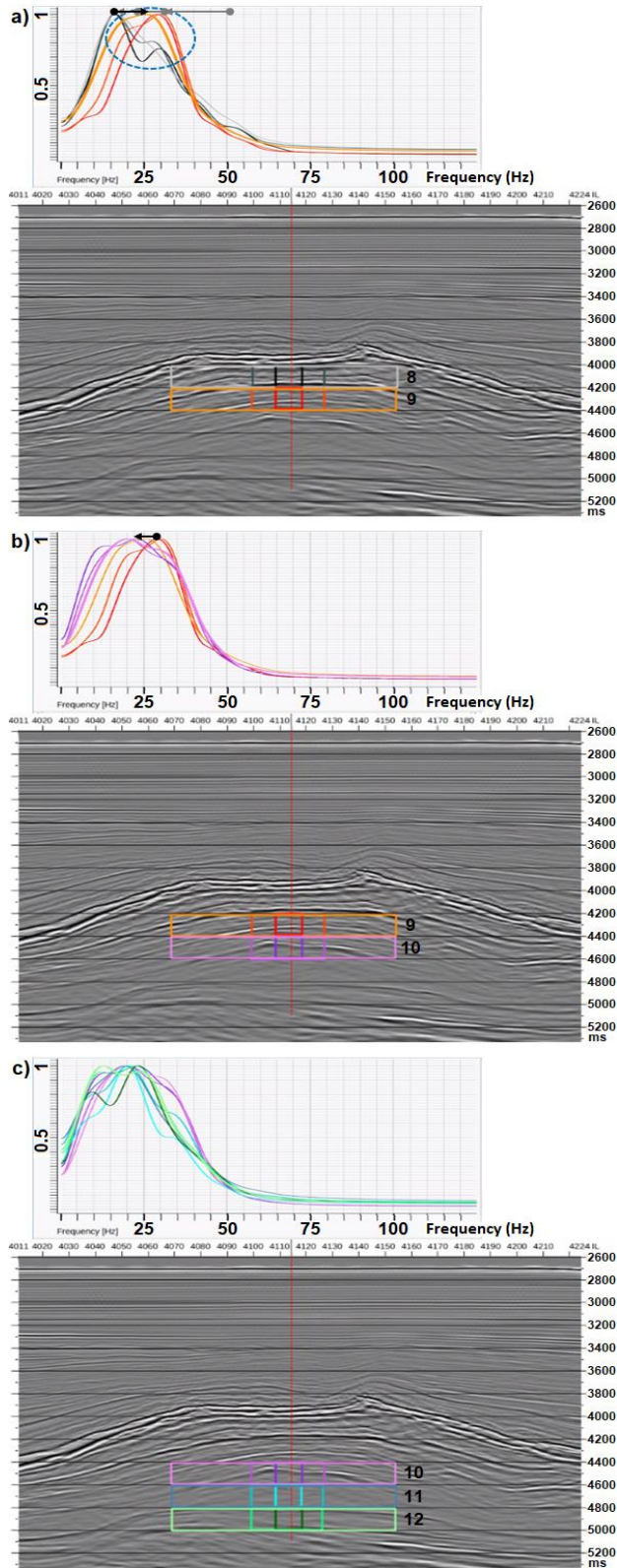


Figure 7: Normalized frequency spectrum comparing the frequency bands from: a) layer 8 and 9; b) layer 9 and 10 and; c) layer 10, 11 and 12. For each layer, frequency bands of 3 analysis windows of different widths (10, 30 and 85 traces) are calculated. The windows position are marked over the TWT seismic section.

Discussion

The preliminary results of the spectrum analysis performed in this seismic section from Buzios oil field have shown that peak frequencies move from, approximately, 50 Hz to 15 Hz from sea bottom to the last layer respectively. Most part of high frequency loss has been occurred in post-salt package, specifically from 5th to 6th layer (3600 to 3800 ms) (Figure 6b and Figure 8).. After that, higher frequency content is lost slowly from 6th up to the last layer. Based on well data we can identify that layer 6 interval is represented by shales and marls (Figure 8). These results are in alignment with other authors which describe high attenuation (low Q values) related to shales (Klimentos and McCann, 1990; Piane et al., 2014) and marls (Levergne, 1986).

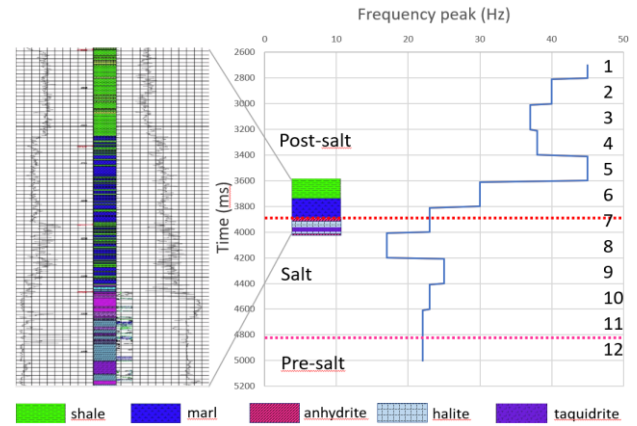


Figure 8: Profile showing frequency peak vs time for each layer interval. Colored blocks over the graph illustrates the lithology identified in layer 6 and layer 7 interval based on composite profile on the left.

The high frequency recovery from 8th to 9th (4200 ms to 4400 ms) layer may be an evidence of apparent attenuation due to thin layers effect – the stratigraphic filtering (Banik et al. 1985; Resnick, 1990) – occurred in layer 7 and layer 8, if this is related to a real physical phenomenon. However, it can also be related to bad migration velocity, as was assumed a constant velocity of 4500 m/s for the entire salt layer in the migration model (Figure 2). Evaluating the seismic image, we can easily observe important salt stratification, what is a strong indication of physical property changes inside the salt. Further analysis will be conducted to define if it is related to real physical phenomena or if it is related to some data processing issue.

Conclusions

Most part of high frequency loss has been occurred in post-salt package, specifically from 5th to 6th layer (3600 to 3800 ms) (Figure 6b and Figure 8). This fact may be an indication of strong viscoelastic behavior of the 6th layer which would be related to the presence of shales and marls in this interval. After that, higher frequency content is lost slowly from 6th up to the last layer, suggesting reduced intrinsic attenuation from layer 7 down to layer 12 (3800 to 5000 ms).

High frequency recovery in the salt layer may be an evidence of apparent attenuation due to thin layer effect occurred in the layer 8.

Very slight frequency variation between 9th and 12th layers (4200 ms to 5000 ms) indicates low intrinsic attenuation of the formations in this interval – located in the salt dome – dominated by halite. Despite the salt layer present relatively strong reflection due to the high impedance contrast between clastic-salt contacts, salt-carbonate contacts and contacts between salt of different compositions (i.e. halite, anhydrite, taquidrite), what causes severe reduction of signal amplitudes, the preliminary results of the present study have shown that the salt preserves frequency content. It means that the salt layer does not present significant viscoelastic behavior.

The insignificant variation in frequency bands between last salt layer (close to the base of the salt (11th layer) and first layer inside pre-salt formation (12th layer)) and the inexpressive loss in the 12th layer also suggests that the pre-salt formation at this level presents a behavior predominantly elastic. Moreover, no significant high and low frequency variations in horizontal direction (among 3 analysis windows of 10, 30 and 85 traces) for layers 2, 3, 4, 5, 7, 8, 10, 11 and 12 indicates that intrinsic attenuation is horizontally homogeneous in these layers. Just layers 6 and 9 have shown some attenuation anisotropy in horizontal direction.

It is important to highlight that these conclusions are based in preliminary results of spectrum analysis of one seismic section extracted from a 3D seismic volume of Búzios field. Thus, to confirm that the characteristics and behavior of the signal frequency variation observed here is related to a local or regional behavior, similar analysis will be carried out in other seismic lines and crosslines of the referred PSDM seismic cube.

It is also important to consider that some not efficient processing steps as stacking, debubble or even the migration may artificially modify the wavelet form and consequently the frequency band calculation. Due to these facts, spectral analyses of pre-stack data are planned to be conducted to eliminate/reduce the influence of possible alterations in the frequency band caused by some processing methods. Additionally, Q factor estimation in both post-stack and pre-stack seismic data will be performed to quantify attenuation.

Acknowledgments

This study has been supported by Petrobras Research Center (CENPES) and the Seismic Inversion and Seismic Imaging Group (GISIS) from Fluminense Federal University (UFF – RJ, Brazil). The first author would like to thank CAPES for the PhD scholarship and GISIS team for the prolific technical discussions. And also, thanks Emerson for the academic licenses of the Paradigm software and for the provided technical support.

References

BEST, A. I. and McCANN, C. 1995. Seismic attenuation and pore-fluid viscosity in clay-rich reservoir sandstones. *Geophysics*, 60 (5), p. 1386–1397.

BANIK, N. C., LERCHE, I. and SHUEY, R. T. 1985. Stratigraphic filtering, Part I: Derivation of the O'Doherty-Anstey formula. *Geophysics*, 50(12), p. 2768 – 2774.

BATZLE, M., HOFMANN, R., PRASAD, M., KUMAR, G., DURANTI, L. and HAN, D. 2005. Seismic Attenuation: Observations and Mechanisms. SEG Houston 2005 Annual Meeting. Expanded Abstract. RP 4.1, p. 1565-1568.

KLIMENTOS, T. and McCANN, C. 1990. Relationship among compressional wave attenuation, porosity, clay content, and permeability in sandstones. *Geophysics*, 44(8), p. 998-1014.

KUTEYNIKOVA, M., TISATO, N., RUBINO, G., and QUINTAL, B. 2012. Numerical and laboratory measurements of seismic attenuation in partially saturated rocks. SEG Las Vegas 2012 Annual Meeting. Expanded Abstract. p. 1-6.

LEVERGNE, M. 1989. *Seismic Methods*. Institut français du pétrole publications. Ed. Technip.

MOREIRA, J. L. P., Madeira, C.V., Gil, J.A., e Machado, M.A.P. 2007. Bacia de Santos. *Boletim de Geociencias da PETROBRAS*, v. 15, n. 2, p. 531–549.

MADONNA, C., TISATO, N., BOUTAREAUND, S., and MAINPRICE, D. 2010. A new laboratory system for the measurement of low frequency seismic attenuation. SEG Denver 2010 Annual Meeting. Expanded Abstract. p. 2675-2680.

MULLER, T. M., GUREVICH, B., and LEBEDEV, M. 2010. Seismic wave attenuation and dispersion resulting from wave-induced flow in porous rocks – A review. *Geophysics*, 75(5), p. 75A147-75A164.

PIANE, C. D., SAROUT, J., MADONNA, C., SAENGER, E. H., DEWHURST, D. N., and REAVEN, M. 2014. Frequency-dependent seismic attenuation in shales: experimental results and theoretical analysis. *Geophys. J. Int.*, 198, p. 504–515.

PRASAD, M. and MEISSNER, R. 1992. Attenuation mechanisms in sands: laboratory versus theoretical (Biot) data. *Geophysics*, 57(5), p. 710-719.

PRIDE, S. R., BERRYMAN, J. G. and HARRIS, J. M. 2004. Seismic attenuation due to wave-induced flow. *Journal of Geophys. Research*. 109, B01201.

RESNICK, J. R. 1990. Stratigraphic filtering. *Pageoph*. 132(1-2), p. 49-65.

TISATO, N., MADONNA, C., ARTMAN, B. and SAENGER, E. H. 2011. Low frequency measurements of seismic wave attenuation in Berea sandstone. SEG San Antonio 2011 Annual Meeting. Expanded Abstract. p. 2277-2281

TOKSÖZ, M. N., JOHNSTON, D. H. and TIMUR, A. 1979. Attenuation of seismic waves in dry and saturated rock: I. Laboratory measurements. *Geophysics*, 44(4), p. 681-690.